ANISOTROPY OF MAGNETIC SUSCEPTIBILITY STUDY OF KAOLINITE MATRIX SUBJECTED TO BIAXIAL TESTS

ANIRUDDHA SENGUPTA*

Department of Civil Engineering, Indian Institute of Technology, Kharagpur 721302, India

Abstract—The potential for structural failure of consolidated clay materials, which is of great importance in many applications, typically are assessed by measuring the localized strain bands that develop under anisotropic load stress. Most methods are precluded from providing a full understanding of the strain anisotropy because they only give two-dimensional information about the stressed clay blocks. The purpose of the present study was to investigate three-dimensional strain localization in a kaolinite matrix, caused by strain anisotropy due to a biaxial plane-strain test, using a relatively new method known as Anisotropy of Magnetic Susceptibility (AMS). This method involves induction of magnetism in an oriented sample in different directions and measurement of the induced magnetization in each direction. The AMS analyses were performed on core samples from different parts of the deformed kaolinite matrix. The degree of magnetic anisotropy (P'), which is a measure of the intensity of magnetic fabric and a gauge of strain intensity, was shown to be greater in cores containing shear bands than in those containing none. A threshold value for P' for the deformed kaolinite matrix was identified, above which shear bands may develop. The comparison of the shape parameter (T), obtained from undeformed and deformed samples, illustrated a superimposition of prolate strain over the original oblate fabric of the kaolinite matrix. The orientation of the principal strain axis revealed that reorientation or rotation of the principal axis occurred along the shear bands.

Key Words—Anisotropy of Magnetic Susceptibility, Biaxial Test, Kaolinite, Strain Localization.

INTRODUCTION

In many materials subjected to extreme loading conditions, the initially smooth distribution of strain changes to being very localized. Typically, the strain increments progressively concentrate damage in narrow zones which induce 'shear bands', while most of the material seems undamaged. Such strain localization can be induced by geometrical effects (*e.g.* necking of metallic bars) or by material instabilities (*e.g.* micro-cracking, frictional slip, or plastic flow). The formation of such localized regions of high strain occurs in a variety of materials, *e.g.* polycrystalline structural metals, soils, rocks, ductile single crystals, polymers, and other solids (Vardoulakis, 1980; Sengupta and Sengupta, 2004; Zuev *et al.*, 2003; Duszek-Perzyna and Perzyna, 1996). The emergence of shear bands is a precursor to structural failure. Shear bands may denote weak areas or areas of plastic flow and are accompanied by strain rates which are orders of magnitude greater than strain rates found in other parts of the material. The accumulation of strain in this narrow zone is primarily responsible for the accelerated softening response exhibited by many materials at post-peak strength (Chu *et al.*, 1996; Read and Hegemier, 1984).

Various methods, such as X-ray diffraction (Balasubramanium, 1976; Nemat-Nasser and Okada., 2001), radiography (Arthur *et al.*, 1977), stereophotogrammetry (Desrues *et al.*, 1996; Finno and Rhee., 1993; Finno *et al.*, 1997), digital-image processing (Liang *et al.*, 1997; Dudoignon *et al.*, 2004), and scanning and transmission electron microscopy (SEM/TEM) (Hicher *et al.*, 1994), have been used by researchers to track particle arrangement, damage, and shear-band formation in laboratory experiments.

The Anisotropy of Magnetic Susceptibility (AMS) methods have been used to analyze the fabric of metamorphic and sedimentary rocks since 1960. Good correlation exists between the orientations of the principal axes of the susceptibility ellipsoid and the orientations of the principal axes of the strain ellipsoid in deformed rocks (Hrouda and Janak, 1976; Rathore, 1979; Hrouda, 1993; Tarling and Hrouda, 1993; Borradaile and Tarling, 1981). The degree of magnetic anisotropy has been correlated with the magnitude of strain for different minerals (Hrouda, 1993; Mukherji *et al.*, 2004; Sen *et al.*, 2005) and many studies have used AMS data to analyze the strain (Borradaile and Tarling 1981, 1984; Mukherji *et al.*, 2004). While conventional methods of analysis generally provide information about 2-D strain, AMS analysis gives information about strain in three dimensions. Compared to the conventional methods, AMS analysis also has the advantage of being a relatively quick method for determining mineral preferred orientations. Therefore, in the present investigation, the anisotropy of particle arrangement, due to the

* E-mail address of corresponding author:
sengupta@civil.iitkgp.ernet.in

intensity of strain in a sheared clayey matrix, was investigated by measuring the degree of magnetic anisotropy. The experimental study was performed on kaolinite test specimens consolidated and sheared during an undrained biaxial test. The kaolinite crystals lack interlayer charges and avoid the problems associated with hydration and swelling. Thus the AMS method can be entirely focused on the simple particle rearrangement during the mechanical test.

ANISOTROPY OF MAGNETIC SUSCEPTIBILITY

Every mineral has a susceptibility to magnetization when placed in an external magnetic field. This magnetic susceptibility (K in SI units) of the mineral is related to the induced magnetization (M) to the external magnetic field (H) into which it is immersed by the relationship M = KH. The magnetic susceptibility for a mineral is not the same in every direction, and this is referred to as AMS. The AMS of a mineral may be controlled either by the crystallography of the mineral or by its shape. In most minerals, the induction of magnetism takes place in the direction of the longest crystallographic axis, which is the preferred axis of growth of the crystal. Such anisotropy is referred to as crystallographic anisotropy. In some minerals, however, the AMS is controlled by the shape and this is referred to as shape anisotropy (Tarling and Hrouda, 1993). The use of AMS of minerals has, over the past few decades, been extended to deformed rocks in order to analyze petrofabrics and to gauge the intensity of strain (Borradaile and Alford, 1987; Dehandschutter *et al.*, 2004, 2005). To determine the AMS of a material, the susceptibility of the material to be magnetized, in different directions, is computed, providing a database that is used to identify the zones of strain localization and interpretations of the orientations of the principal directions of the grains in clayey soils.

FUNDAMENTAL PRINCIPLES OF MEASURING AMS IN GEOMATERIALS

In the present study, measurement of AMS was carried out using the Kappabridge apparatus (model KLY-4S with spinning holder) manufactured by AGICO (2003). Since this instrument has a very high sensitivity (on the order of 10^{-8} SI), it is very useful for geomaterials with weak susceptibilities. All samples analyzed in the Kappabridge device comply with the size specifications (core with a diameter of 25.4 mm and a height of 22 mm) and means of measurement.

The apparatus consists of a pick-up unit, control unit, and user's computer and measures the AMS of a slowly spinning specimen. The specimens are adjusted into three perpendicular positions only; measurement is rapid and precise. The KLY-4S Kappabridge (specification give in Table 1) also has the option of use in a static mode where the AMS of an immobile specimen is measured interactively with a computer in 15 different positions, using a rotatable holder. The positions are changed manually and the AMS parameters are determined.

Analyses carried out using the Kappabridge device give rise to the following data related to the three axes of

Table 1. Kappabridge KLY-4S instrument specifications.

For spinning specimen			
Cylinder	Diameter	25.4 mm (+0.2, −1.5)	
	Length	22.0 mm (+0.5, −1.5)	
Cube		20.0 mm (+0.5, −1.5)	
For static specimen			
Cylinder	Diameter	25.4 mm (+1.0, −1.5)	
	Length	22.0 mm (+2.0, −2.0)	
Cube		20.0 mm (+0.5, −2.0)	
Cube		23.0 mm (+0.5, −2.0)	
ODP box		26 mm × 25 mm × 19.5 mm	
Fragments		40 cm^3	
Pick-up coil inner diameter		43 mm	
Nominal specimen volume		10 cm^3	
Operating frequency		875 Hz	
Field intensity		3 Am^{-1} to 450 Am^{-1} in 21 steps	
Field homogeneity		0.2%	
Measuring range		0 to 0.2 (SI)	
Sensitivity (300 Am^{-1})	Bulk measurement	3×10^{-8} (SI)	
	AMS measurement	2×10^{-8} (SI)	
Accuracy within one range		0.1%	
Accuracy of the range divider		0.3%	
Accuracy of the absolute calibration		3%	
HF Electromagnetic Field Intensity Resistance		1 Vm^{-1}	

magnetic susceptibility ellipsoid K_1, K_2, and K_3, where $K_1 \geqslant K_2 \geqslant K_3$:

(a) Magnitudes and orientations of the three principal axes of the magnetic susceptibility ellipsoid (K_1, K_2, and K_3); (b) Mean susceptibility, $K_m = (K_1+K_2+K_3)/3$; (c) Degree of magnetic anisotropy, $P' = \exp \sqrt{\{2[(\eta_1-\eta_m)^2+(\eta_2-\eta_m)^2+(\eta_3-\eta_m)^2]\}}$, where $\eta_1 = \ln K_1$, $\eta_2 = \ln K_2$, $\eta_3 = \ln K_3$, and $\eta_m = (\eta_1.\eta_2.\eta_3)^{1/3}$. This is a measure of the eccentricity of the magnetic susceptibility ellipsoid; (d) Shape parameter, $T = (2\eta_2-\eta_1-\eta_3)/(\eta_1-\eta_3)$; (e) Strength of magnetic foliation, $F = (K_2-K_3)/K_m$; and (f) Strength of magnetic lineation, $L = (K_1-K_2)/K_m$

UNDRAINED BIAXIAL LABORATORY TESTS

Material properties of kaolinite

A commercially available kaolinite was used in the laboratory tests. It is sold in 30 kg polythene bags under the name 'China clay' (M/s. Prabha Minerals, Kolkata, India). The chemical formula of the material is $Al_2Si_2O_5(OH)_4$. Its specific gravity is 2.68. The Liquid Limit, the Plastic Limit, and the Plasticity Index of the kaolinite are 50%, 31%, and 19%, respectively. The activity number (ratio of Plasticity Index to the percentage of clay sizes) of the material is 0.45. The granulometry of the kaolinite shows that 72% of clay particles are <10 μm and 60% are <2 μm (Figure 1), comparable with values for kaolinite found in the literature (*e.g.* Prashant and Penumadu, 2005). The engineering classification of the soil is ML according to the Unified Soil Classification As per Indian code IS: 1498−1970, the soil is classified as a 'CI (clay with intermediate pasticity) material.'

Preparation of the soil samples

The kaolinite clay samples were prepared in a circular slurry tank 450 mm in diameter. The tank, with both ends open, was placed in a sand bath to facilitate drainage of water through the bottom (Figure 2). A uniform slurry of kaolinite was prepared in the tank by mixing kaolinite powder with 155% (by weight) degassed, deionized water. During preparation of the slurry, 2% sodium hexametaphosphate ('Calgon®'), a dispersing agent, was added to the deionized water. In principle, the dispersing agent should only break the clusters of the clay particles and disperse them without affecting the original shape and size of the particles. The slurry thus prepared was allowed to consolidate under a uniform pressure of 276 kPa up to the end of the primary consolidation (15−30 days). Sample preparation was as suggested by Sachan and Penumadu (2007). Fully consolidated and saturated soil samples were extruded from the middle of the tank (to ensure homogeneity) with the help of a rectangular split mold of 150 mm × 75 mm × 30 mm dimensions (Figure 2). The split mold had two halves which locked into position to form a hollow rectangular box for sample extrusion. The two halves were separated for sample recovery. Observation by scanning electron microscopy (SEM) of the extruded, consolidated kaolinite matrix showed the face-to-face arrangement of the clay platelets and their sub-horizontal alignment (Figure 3). This micro-fabric pattern was defined here as an initially consolidated (or dispersed) fabric.

The biaxial laboratory tests

The laboratory biaxial plane-strain test cell consisted of two perspex plates, 226 mm × 146 mm × 25 mm in size, bolted together, with a 140 mm × 70 mm × 25 mm soil specimen, wrapped in a transparent latex membrane, sandwiched between them as shown in Figure 4. The lower platen was restrained from movement. The upper platen could slide smoothly in the vertical direction only between two fixed guides compressing the clay matrix sandwiched between the perspex plates. The kaolinite matrix could deform in the vertical and lateral directions only − deformations to the front and rear (out of plane)
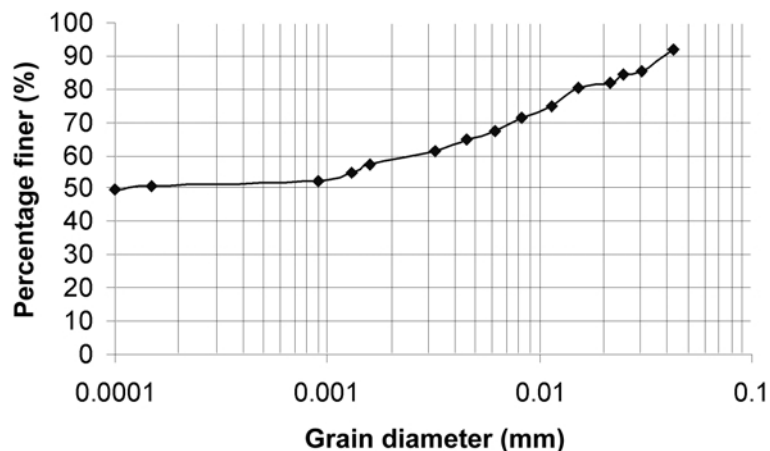

Figure 1. Grain-size distribution of 'China Clay' kaolinite measured by laser granulometry.
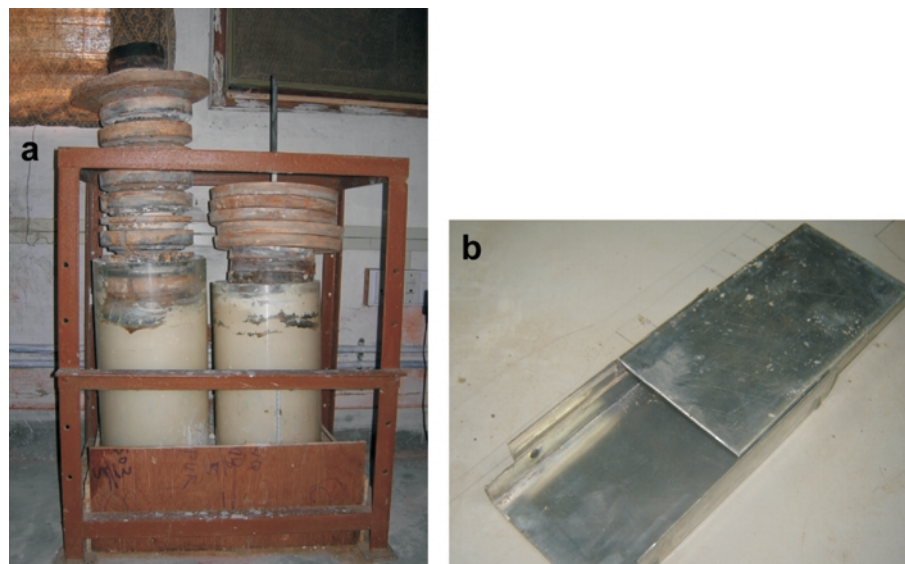
Figure 2. (a) Slurry (or consolidation) tank (450 mm in diameter). The vertical consolidation loads are visible at the top of the perspex tanks. The sand bath is not visible; (b) rectangular split mold (150 mm long, 75 mm wide, and 30 mm thick).

faces were restricted by the two fixed perspex plates. The bottom of the upper platen could be considered to be rough. Before the tests, square grids 10 mm × 10 mm in size were imprinted on the soil samples so that the deformations and locations of the shear bands within the soil sample could be visualized through the transparent membrane and perspex plate and measured during the tests. A stationary digital camera was used to record the deformation of the grids as the axial strain progressed. The average axial stress and deformations in axial and in both horizontal directions were measured with a pressure transducer and Linear Variable Differential
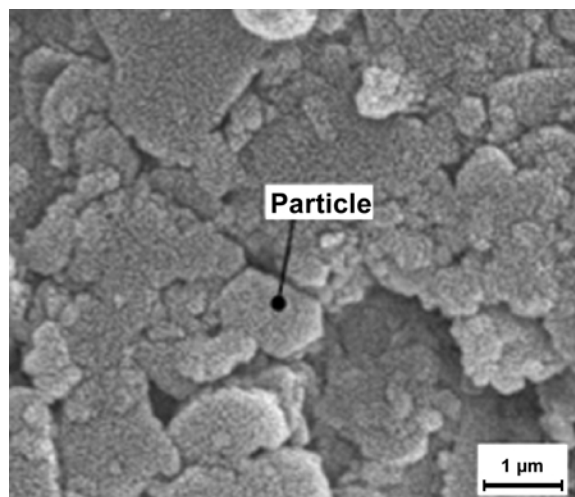

Figure 3. SEM image of the initially consolidated kaolinite matrix (absorbed electron mode) showing the very small size of the kaolinite crystals according to the granulometry curve.

Transformers (LVDTs). The average pore-water pressures at the top and bottom of the sample were also measured with pore-pressure transducers. The inside walls of the perspex sheets were coated with a very thin layer of lubricating oil to reduce friction between the latex membrane and the cell walls. The whole plane-strain device, including soil specimen, was mounted on a triaxial loading frame (Figure 4). Two measuring rulers (one in horizontal and another in vertical directions) were fixed to the device to accurately trace the coordinates of the deformed mesh at different stages of the experiment. The triaxial loading machine was strain controlled. At the beginning of the test, a uniform pressure was first applied pneumatically on two lateral free sides of the kaolinite sample. The sample was allowed to consolidate under the lateral pressures. Once the sample was fully consolidated, it was sheared by lowering the upper loading platen at a constant, slow strain rate of 1.2 mm min^{-1} (at 0.86% strain; Figure 4).

Three biaxial tests were performed on the kaolinite matrix at 70 kPa, 140 kPa, and 210 kPa confining (consolidation) pressures. Note that only three tests at three different confining pressures were needed to determine the material strength parameters for a soil. Each of these tests was carried out up to 14% axial strain level. To identify the differences in the magnitude of localized strain developed in the samples, AMS studies were carried out. The AMS analyses were performed on cylindrical cores taken from the deformed clay matrix (Figure 6) at the end of the biaxial tests, using a cylindrical brass extruder (Figure 5a). To identify variations in strain in different parts of each sheared test sample, five or six cylindrical cores were sampled from the vicinity of the strain locale and away from them
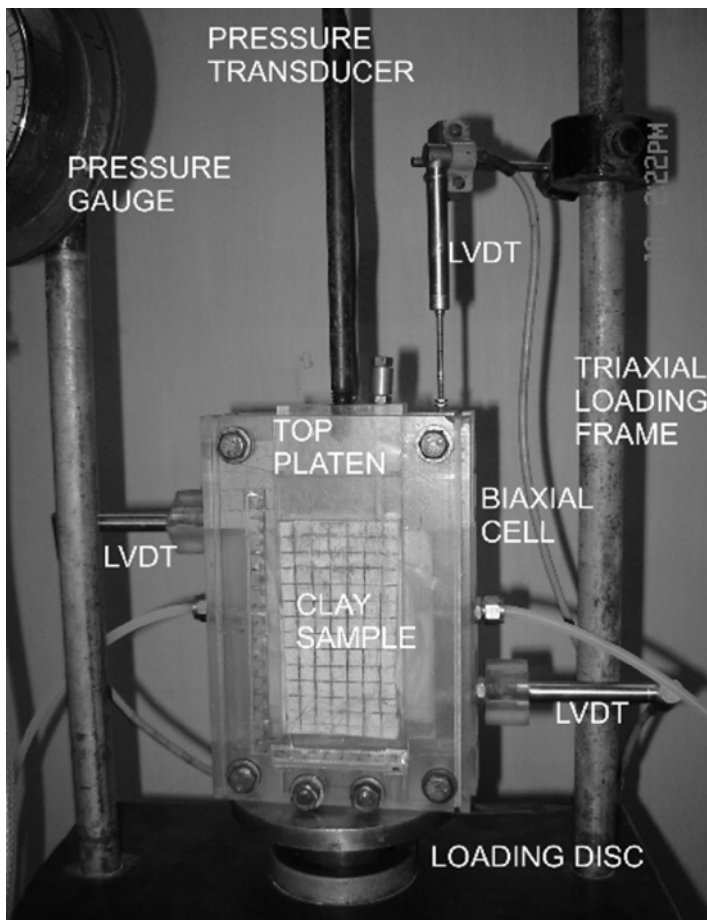
Figure 4. Details of the biaxial cell and biaxial test setup. The kaolinite matrix with imprinted 10 mm × 10 mm grids on it can be seen through the transparent perspex sheet in front of the cell. The LVDTs attached to the sample measure deformation in the vertical and the two free lateral directions. The kaolinite sample is sheared under compressive load imparted by raising the loading disk at the bottom at a constant rate.
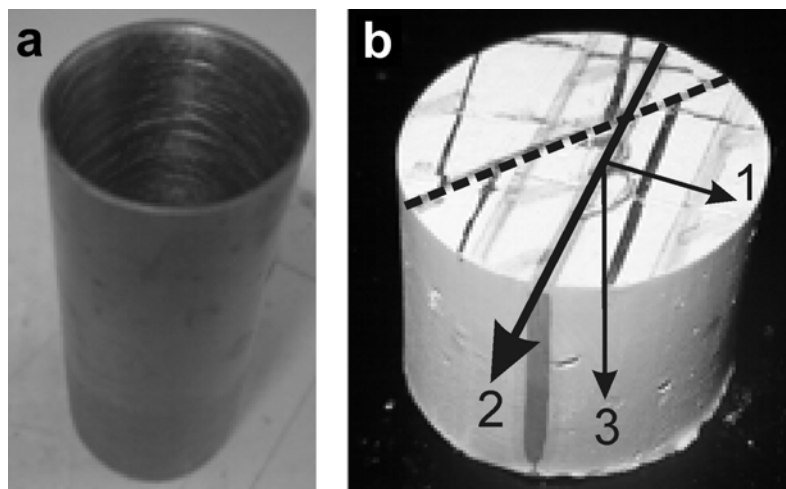

Figure 5. (a) A metallic core extruder; (b) a cylindrical core sampled through the sheared kaolinite matrix. Arrows 1, 2, and 3 are the three reference axes. Axis 1 is the horizontal axis and is orthogonal to the loading direction. Axis 2 indicates the vertical loading direction. Axis 3 is the other orthogonal axis. The shear plane is shown by the shift of the black lines. The core identification number can also be seen on the face of the core.
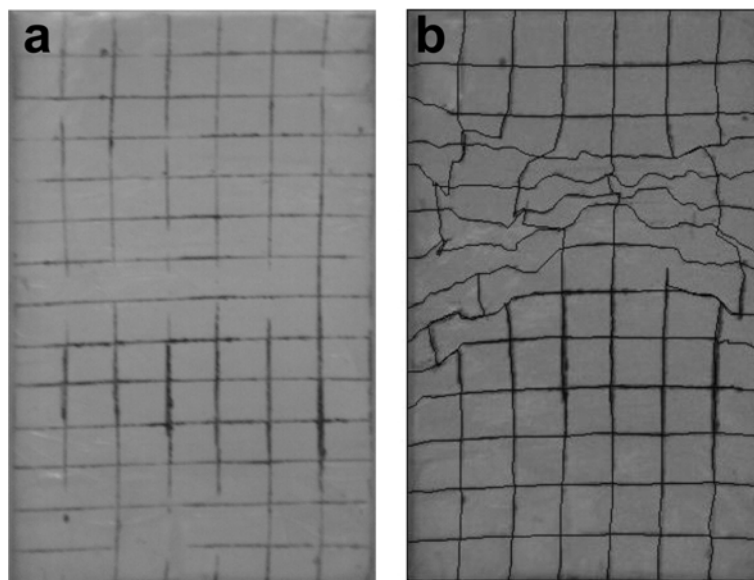
Figure 6. (a) Initially consolidated (before shearing) kaolinite matrix with 10 mm × 10 mm square grids drawn on the test piece; (b) damaged (sheared) test piece after shearing up to 14% axial strain level. The deformed grids show the locations of the sheared zones.

(Figure 7). The core samples from each sheared test piece were subjected to AMS analysis. For comparison, two cylindrical cores from one consolidated, undeformed sample were also analyzed. The objective of the study was to check the difference in the P' value (a measure of strain) and the orientation of the principal direction at the different sampling places of the deformed sample. Each of the cylindrical cores was identified by a unique number so that its location in a particular clay matrix could be found at any time. The vertical loading direction is marked by axis 2 in each core (Figure 5b, where the reference axes are also shown). All the AMS analyses were performed in the spinner mode of the Kappabridge device. After the analyses, Jelinek plots (of P' vs. T) (Figure 8) as well as P' vs. L (Figure 9), P' vs. F (Figure 10), and L vs. F (Figure 11) were prepared in order to identify the shape of the magnetic susceptibility ellipsoid and the strength of the magnetic lineation and magnetic foliations, *etc*.

for the cylindrical cores located at the shear bands and away from them. For comparison, the corresponding parameters for the cores taken from the consolidated, but undeformed, kaolinite matrix were also examined.

RESULTS

In all the laboratory tests reported here, strain localizations were initiated at ~6% strain, irrespective of the confining (consolidation) pressure, before the peak stress was reached. At ~8−10% of axial strain, a single band became prominent and emerged from one of the corners of the upper platen. At 11% axial strain, a conjugate band emerged from the other corner of the upper platen. At ~14% axial strain, formation of the shear bands was complete, and stresses and pore-water pressure values decreased to a threshold residual value, depending on the confining pressure. An undeformed (consolidated) clay matrix and a sheared clay matrix

Table 2. AMS results for the cores from the biaxial test at 70 kPa lateral pressure.

Core no.	Mean susceptibility (K_m), (SI)	L	F	P'	T	K_3
1	$103.8 \times 10{-}6$	1.133	1.389	1.598	0.450	149/77
2	38.93×10^{-6}	1.016	1.097	1.124	0.711	189/54
3	39.69×10^{-6}	1.036	1.099	1.144	0.460	210/60
4	61.65×10^{-6}	1.273	1.285	1.635	0.319	220/72
5	37.32×10^{-6}	1.026	1.080	1.112	0.496	203/62
6	38.59×10^{-6}	1.003	1.084	1.100	0.920	185/60

Cores 1 and 4 are located within shear zones. K_3 is measured in terms of dip direction and dip with respect to the vertical loading axis (0, 0).
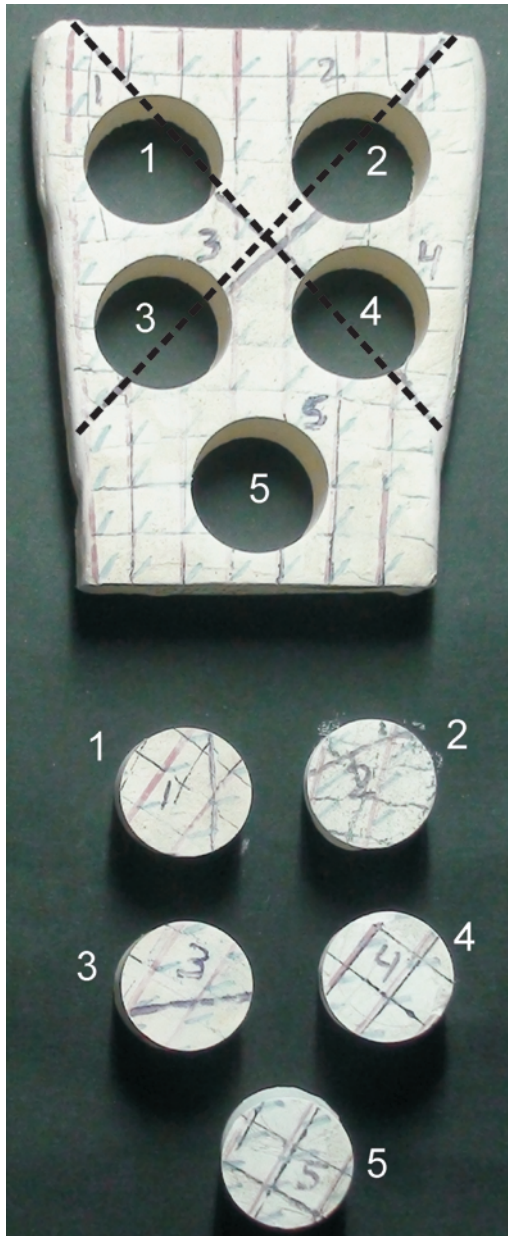
Figure 7. Location of the cylindrical core samples taken from a deformed (sheared) kaolinite matrix. The shear bands formed during shearing are shown by black lines. Cores 2 and 5 are located outside the sheared zones while cores 1, 3, and 4 are within the sheared zones.

with a typical pattern of strain localizations captured in a biaxial test showed that deformations during shearing of the test pieces were evident from the deformation of the 10 mm × 10 mm square grids imprinted on the samples (Figure 6).

The results of measurements on the different cylindrical core samples may be grouped in accordance with the locations of the cores taken from within the strain localization zones and from outside those localization zones (Tables 2−4).

The cylindrical cores extracted from the deformed samples after the biaxial tests (locations shown in Figure 7) were subjected to a magnetic field intensity of 300 A/m in order to measure their magnetic properties. The information obtained (Tables 2−4) included K_m, L, F, P', T, and K_3 for the cores taken from the biaxial tests performed at confining pressures of 70 kPa, 140 kPa, and 210 kPa, respectively. K_3 is shown in Figure 5b in terms of dip direction and dip measured with respect to the vertical loading axis (Axis 2). For comparison, the same data for the cores taken from an undeformed kaolinite sample are also presented (Table 5).

The K_m, P', F, and L values of deformed kaolinite were greater than the values for the undeformed sample. The shape parameter (T) of the undeformed sample is between 0.773 and 0.808 (Table 5). The T values for the cores from sheared zones were between 0.319 and 0.878. For the cores taken from outside the sheared zones in deformed samples, the T values were between 0.325 and 0.824. An important observation is that in all the tests, the P' values of cores containing strain localization are found to be greater than the cores collected from outside localization zones. The P' value, which measures the eccentricity of the magnetic susceptibility ellipsoid and gives a notion of strain, was between 1.054 and 1.066 for the undeformed sample (Table 5); between 1.253 and 1.635 for cores collected from the sheared zones; and between 1.1 and 1.23 for the cores obtained from outside sheared zones in deformed samples. Similarly the value of L, a measure of the intensity of lineation, is 1.006 for the consolidated undeformed sample, between 1.012 and 1.273 for the cores obtained from the sheared zone, and between 1.003 and 1.05 for the cores obtained from outside the sheared zones in the deformed samples. The F value, the strength of foliation, was between 1.043 and 1.054 for the cores obtained from the consolidated but undeformed sample; between 1.063 and 1.389 for the cores from the sheared zones; and, for the cores from outside the sheared zones, between 1.08 and 1.186. The value of the mean susceptibility, K_m, varied from 26.13×10^{-6} to 27.44×10^{-6} for the consolidated undeformed sample, but varied from 41.84×10^{-6} to 103.8×10^{-6} for the cores obtained from the sheared zones and from 33.69×10^{-6} to 40.34×10^{-6} for the cores located outside the sheared zones. The AMS parameters show some scattering of values from core sample to core sample (Tables 2−5). One possible reason for this is the large size of the core samples compared to the size of the clay fabric and the width of the strain localization zones.

A Jelinek Plot of P' vs. T for all the core samples (Figure 8) revealed that all the cores located within the localization zones have P' values which are $\geqslant 1.25$. The plots of L vs. P', F vs. P', and L vs. F (Figures 9−11, respectively) illustrate that both lineation and foliation
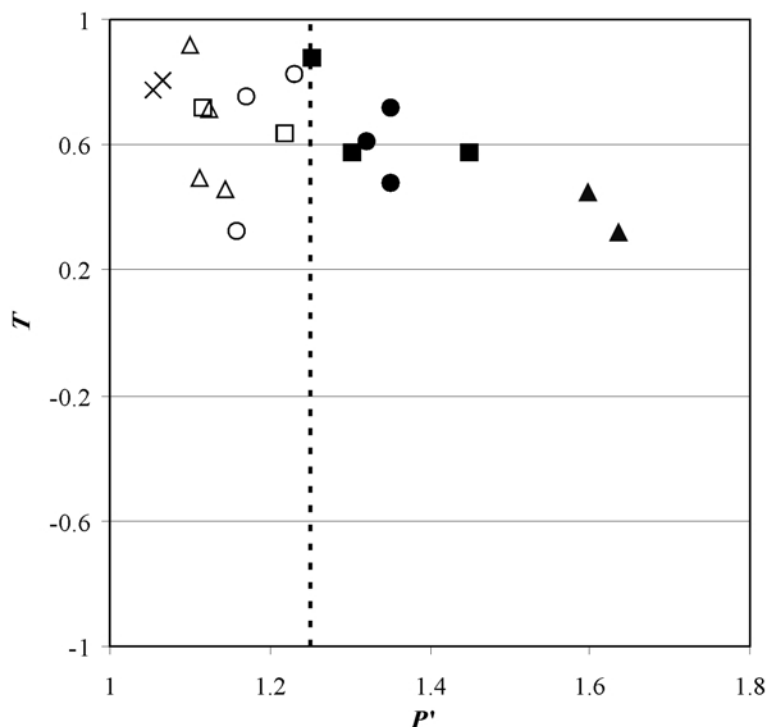
Figure 8. Representation of the shape parameter, *T*, *vs.* the degree of magnetic anisotropy, *P'*, for initially consolidated undeformed matrix (×), for consolidated at 70 kPa and sheared matrix outside the sheared zones (△), for consolidated at 70 kPa and sheared matrix within the sheared zones (▲), for consolidated at 140 kPa and sheared matrix outside the sheared zones (□), for consolidated at 140 kPa and sheared matrix within the sheared zones (■), for consolidated at 210 kPa and sheared matrix outside the sheared zones (○), and for consolidated at 210 kPa and sheared matrix within the sheared zones (●).

increase in strength during shearing of the kaolinite matrix. During the consolidation process, the increase in strength of the foliation is more prominent than the increase in strength in lineation.

The orientation of the principal strain axis in the core samples, as obtained from the AMS analysis, is given by K_3 (Tables 1−4). The K_3 value is stated in terms of dip direction and dip. It is measured with respect to the vertical loading axis (Axis 2 in Figure 5b) of the samples. In Figure 12, the orientation of the strain ellipsoids (K_3) at different locations of the deformed samples (where cores were taken) are plotted and compared with the orientation of the shear bands

(shown as dashed lines) observed during the laboratory tests. Table 6 shows a comparison of the range of K_1 values obtained from the AMS study and the observed inclination of the shear bands in the three laboratory tests. Figure 12 and Table 6 show reorientations of clay platelets along the shear bands.

DISCUSSION

Shear-band propagation in clay has been studied experimentally in the past (Saada *et al.*, 1994; Viggiani *et al.*, 1994; Topolnicki *et al.*, 1990). Large strain concentrations/strain localizations are known to lead to

Table 3. AMS results for the cores from the biaxial test at 140 kPa lateral pressure.

Core. no	Mean susceptibility (K_m), (in SI)	*L*	*F*	*P'*	*T*	K_3
1	38.14×10^{-6}	1.014	1.091	1.116	0.719	170/60
2	69.66×10^{-6}	1.054	1.219	1.303	0.577	214/80
3	41.84×10^{-6}	1.012	1.208	1.253	0.878	228/78
4	40.34×10^{-6}	1.035	1.164	1.219	0.635	159/47
5	65.12×10^{-6}	1.077	1.320	1.449	0.578	140/80

Cores 2, 3, and 5 are located within shear zones. K_3 is measured in terms of dip direction and dip with respect to the vertical loading axis (0, 0).
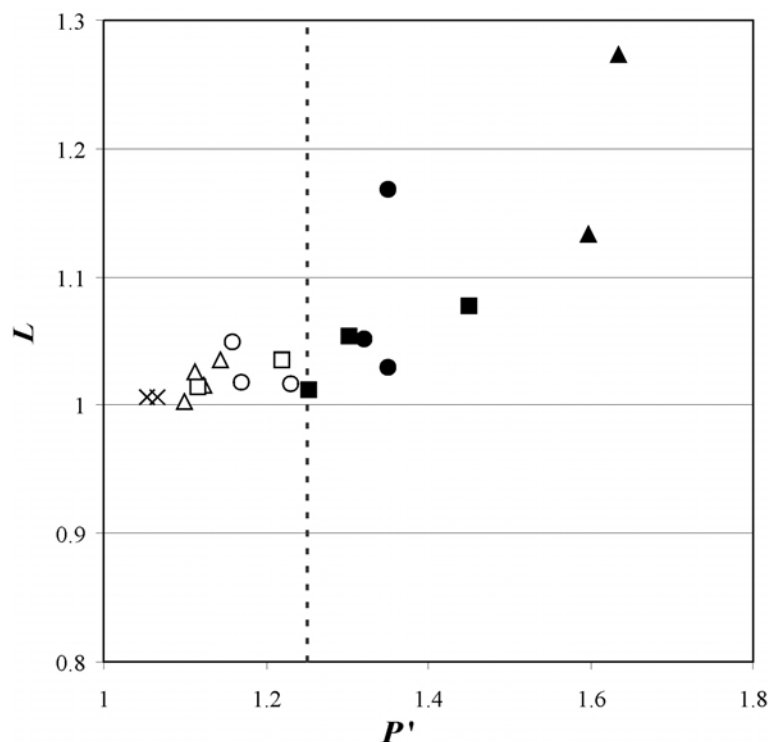
Figure 9. Representation of the strength of magnetic lineation, *L*, *vs.* the degree of magnetic anisotropy, *P'*, for initially consolidated undeformed matrix (×), for consolidated at 70 kPa and sheared matrix outside the sheared zones (△), for consolidated at 70 kPa and sheared matrix within the sheared zones (▲), for consolidated at 140 kPa and sheared matrix outside the sheared zones (□), for consolidated at 140 kPa and sheared matrix within the sheared zones (■), for consolidated at 210 kPa and sheared matrix outside the sheared zones (○), and for consolidated at 210 kPa and sheared matrix within the sheared zones (●).

the development of shear bands in clays (Tchalenko, 1968; Dehandschutter, 2004, 2005), implying that the magnitude of strain would be greater in the vicinity of shear bands than away from them. The AMS data from the sheared kaolinite matrix reveal a greater P' value in core samples taken from within shear bands than those taken from elsewhere (Figure 8). The P' value is far greater in deformed than in undeformed samples. Therefore, AMS data are clearly useful in gauging strain-intensity variations in the kaolinite matrix investigated. A minimum P' value of 1.25 is needed for the development of shear bands in the kaolinite. This

threshold value of P' is highlighted by the dashed line in Figure 8, implying that all the samples with $P' > 1.25$ could develop shear bands, after which they fail. This threshold P' value of 1.25 is critical for the kaolinite matrix used in the present experiments and can be considered analogous to the ultimate strength of the material beyond which it experiences structural failure.

The difference in the shape parameter (T) between the undeformed and deformed samples is also revealing. The T value of 0.773 for the undeformed sample (Table 4) indicates a strong oblate shape of the magnetic susceptibility ellipsoid in the sample, on account of the

Table 4. AMS results for the cores from the biaxial test at 210 kPa lateral pressure.

Core no.	Mean susceptibility (K_m), (SI)	L	F	P'	T	K_3
1	34.47×10^{-6}	1.050	1.100	1.158	0.325	190/79
2	48.21×10^{-6}	1.030	1.195	1.351	0.717	219/85
3	48.44×10^{-6}	1.168	1.063	1.350	0.477	143/77
4	34.34×10^{-6}	1.018	1.135	1.170	0.753	185/78
5	42.98×10^{-6}	1.052	1.234	1.320	0.609	209/87
6	33.69×10^{-6}	1.017	1.186	1.230	0.824	179/73

Cores 2, 3, and 5 are located within shear zones. K_3 is measured in terms of dip direction and dip with respect to the vertical loading axis (0, 0).
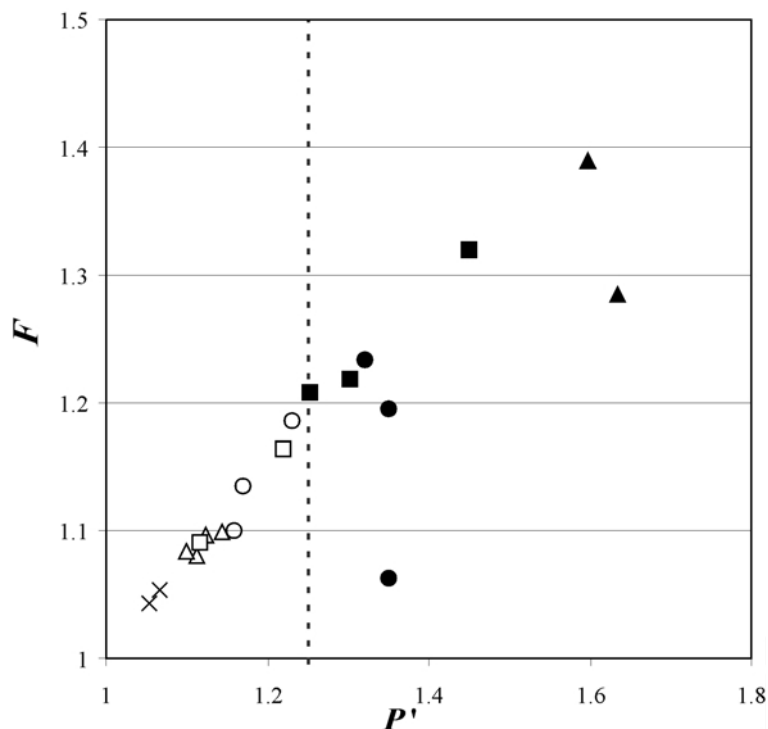
Figure 10. Representation of the magnetic foliation, *F*, *vs.* the degree of magnetic anisotropy, *P′*, for initially consolidated undeformed matrix (×), for consolidated at 70 kPa and sheared matrix outside the sheared zones (△), for consolidated at 70 kPa and sheared matrix within the sheared zones (▲), for consolidated at 140 kPa and sheared matrix outside the sheared zones (□), for consolidated at 140 kPa and sheared matrix within the sheared zones (■), for consolidated at 210 kPa and sheared matrix outside the sheared zones (○), and for consolidated at 210 kPa and sheared matrix within the sheared zones (●).

flat orientation of the fabric in the blocks that were obtained from the kaolinite slurry after consolidation under static loads (Figure 3). Therefore, the *T* parameter quantifies the shape of the pre-deformational kaolinite block and is similar to a fabric that natural clay would acquire when it is consolidated under its own load in nature. On plane-strain deformation, the *T* value of the kaolinite generally falls below 0.773, indicating that, as the undeformed sample was subjected to shearing in the biaxial cell, a superimposition of prolate strain over the original oblate fabric of the kaolinite block occurred, leading to reduction of the *T* value. Similar superimposition has also been interpreted and modeled for sedimentary thrust sheets (Hrouda, 1991) and for deformations associated with diagenesis (Hrouda and Ježek, 1999). In three cores taken from sheared samples, *T* is >0.773, which indicates flattening of the original oblate fabric. From the experimental work of Kapicka *et al.* (2006) on marls, an increase in strain is known to lead to greater reorientation of the phyllosilicates in them. Moreover, Hicher *et al.* (1994) also documented reoriented particles along shear bands and failure surfaces in clays. In light of these studies, the *T* value of the kaolinite matrix after deformation is inferred to depend on the direction in which reorientation of the clay minerals took place. A reorientation in a direction perpendicular to the original flattening fabric would be equivalent to superimposition of prolate fabric over the original oblate one, thus leading to a *T* value of <0.773. On the contrary, if the deformation was to lead to reorientation in a direction parallel to the original oblate fabric, then further flattening of the initial fabric would

Table 5. AMS results for the cores obtained from the undeformed kaolinite sample.

Core no.	Mean susceptibility (K_m), (SI)	*L*	*F*	*P′*	*T*	K_3
1	27.44×10^{-6}	1.006	1.043	1.054	0.773	160/47
2	26.13×10^{-6}	1.006	1.054	1.066	0.808	170/50

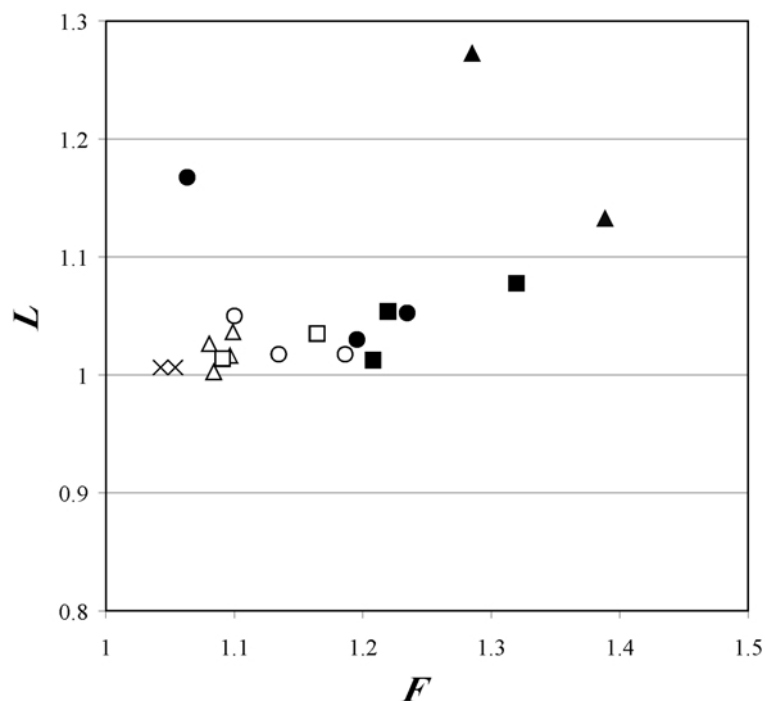K_3 is measured in terms of dip direction and dip with respect to the vertical loading axis (0, 0).

Figure 11. Representation of the strength of magnetic lineation, *L*, *vs.* magnetic foliation, *F*, for initially consolidated undeformed matrix (×), for consolidated at 70 kPa and sheared matrix outside the sheared zones (△), for consolidated at 70 kPa and sheared matrix within the sheared zones (▲), for consolidated at 140 kPa and sheared matrix outside the sheared zones (□), for consolidated at 140 kPa and sheared matrix within the sheared zones (■), for consolidated at 210 kPa and sheared matrix outside the sheared zones (○), and for consolidated at 210 kPa and sheared matrix within the sheared zones (●).

be observed, resulting in a *T* value >0.773. Because shear bands have developed in the deformed clays, strain at the scale of observation was clearly heterogeneous and strain partitioning has taken place. The reorientation of the minerals was, therefore, different in different parts of the clay block leading to differences in *T* values. However, *P′* values are greater in the cores that contain shear bands than in those which do not, indicating the usefulness of AMS data as a strain proxy in clays. Figures 9–11 show that both lineation and foliation increase during shearing, but, during the consolidation process, the increase in foliation is significantly greater than the increase in lineation, which means that the material experienced compaction and no shearing during the consolidation process. The reorientation of the principal strain direction during strain localization is also revealed by the AMS study (Figure 12, Table 6). The orientation of the principal strain axis (Table 6)

from the cores taken from the undeformed sample and outside the localization zones is between 70° and 80° to the vertical axis, *i.e.* very close to the horizontal plane. The principal strain axis for the cores taken from the strain localization zones show reorientation along the shear-band inclinations, observed during the biaxial tests. The orientation of the principal axis is between 22° and 45°. These values are found to be reasonably comparable with the observed values (38°–43°) for the inclinations of shear bands in the biaxial tests. Figure 12 compares the orientation of the shear bands (shown as dashed lines) and the orientation of strain ellipsoids at different locations of the deformed samples from the three biaxial tests. The re-orientation of clay platelets along the shear-band zones are also shown. The scattering of the AMS data (Tables 1–5, Figures 8–12) could be due to a number of reasons. During extrusion of samples for biaxial testing and AMS

Table 6. Average K$_1$ values of the cores and average inclination of shear bands.

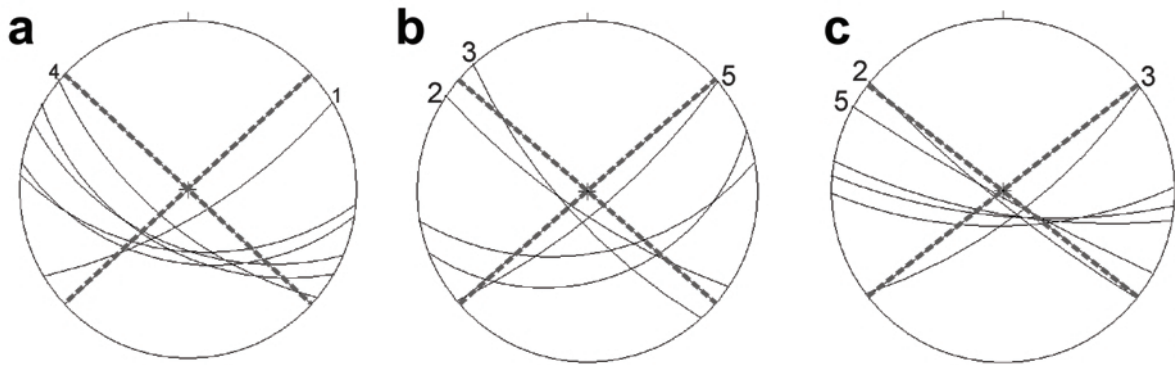| Test no.	Confining pressure (kPa)	Range of K$_1$ (°) from the AMS study		Value (°) of shear-band inclination
		Within localization zones	Outside localization zones	
1	70	33–43	71–80	43
2	140	27–43	71–72	41
3	210	22–45	70–79	38

Figure 12. Stereoplot of the orientation of clay fabrics (K$_3$) obtained from an AMS study of core samples and that for the shear bands (shown as dashed lines) measured in laboratory biaxial shear tests for (a) 70 kPa, (b) 140 kPa, and (c) 210 kPa. The curves showing the orientation of the fabric in the cores containing the shear bands are identified by their corresponding core numbers given in Tables 2, 3, and 4.

study, the samples could have been disturbed, inducing unwanted changes in the microfabric. The thickness of the shear bands has been reported to be between 10 (Scarpelli and Wood, 1982) and 16 times (Vardoulakis *et al.*, 1985) the average grain diameter, implying that the thickness of shear bands could be only ~0.02 mm. The fabric orientations along the shear bands with 25.4 mm cores are, therefore, difficult to measure. The AMS essentially finds the average strains and fabric orientations within the whole core, but most of the data suggest at least qualitative accuracy. The AMS is found to be a useful tool in investigating internal mechanisms such as reorientation/rotation of the principal axis, the change in shape of the grains, *etc.*, associated with strain localizations in soils devoid of strain markers and which cannot otherwise be observed.

REFERENCES

AGICO (2003) *KLY-4/KLY-4S/CS-3/CS-L: User's Guide, Modular system for measuring magnetic susceptibility, anisotropy of magnetic susceptibility, and temperature variation of magnetic susceptibility*. Version 1.1, Advanced Geoscience Instrument Co., Brno, Czech Republic.

Arthur, J.R.F., Dunstan, T., Al-Ani, Q.A.J.L., and Assadi, A. (1977) Plastic deformation and failure in granular media. *Geotechnique*, **27**, 53−74.

Balasubramanium, A.S. (1976) Local strains and displacement patterns in triaxial specimens of saturated clay. *Soils and Foundations*, **16**, 101−114.

Borradaile, G.J. and Alford, C. (1987) Relationship between magnetic susceptibility and strain in laboratory experiments. *Tectonophysics*, **133**, 121−135.

Borradaile, G.J. and Tarling, D.H. (1981) The influence of deformation mechanisms on magnetic fabrics in weakly deformed rocks. *Tectonophysics*, **77**, 151−168.

Borradaile, G.J. and Tarling, D.H. (1984) Strain partitioning and magnetic fabrics in particulate flow. *Canadian Journal of Earth Sciences*, **21**, 694−697.

Chu, J., Lo, S.-C.R., and Lee, I.K. (1996) Strain softening and shear band formation of sand in multi-axial testing. *Geotechnique*, **46**, 63−82.

Dehandschutter, B., Vandycke, S., Sintubin, M.,

Vandenberghe, N., Gaviglio, P., Sizun, J.-P., and Wouters, L. (2004) Microfabric of fractured Boom Clay at depth: a case study of brittle-ductile transitional clay behavior. *Applied Clay Science*, **26**, 389−401.

Dehandschutter, B., Vandycke, S., Sintubin, M., Vandenberghe, N., and Wouters, L. (2005) Brittle fractures and ductile shear bands in argillaceous sediments: inferences from Oligocene Boom Clay (Belgium). *Journal of Structural Geology*, **27**, 1095−1112.

Desrues, J., Chambon, R., Mokni, M., and Mazerolle, F. (1996) Void ratio evaluation inside shear bands in triaxial sand specimen studied by computed tomography. *Geotechnique*, **46**, 529−546.

Dudoignon, P., Gelard, D., and Sammartino, S. (2004) Cam-clay and hydraulic conductivity diagram relations in consolidated and sheared clay-matrices. *Clay Minerals*, **39**, 267−279.

Duszek-Perzyna, M.K. and Perzyna, P. (1996) Adiabatic shear band localization of inelastic single crystals in symmetric double-slip process. *Archive of Applied Mechanics*, **66**, 369−384.

Finno, R.J. and Rhee, Y. (1993) Consolidation, pre- and post-peak shearing responses from internally instrumented biaxial compression device. *Geotechnical Testing Journal*, GTJODJ, **16**, 496−509.

Finno, R.J., Harris, W.W., Mooney, M.A., and Viggiani, G. (1997) Shear bands in plane strain compression of loose sand. *Geotechnique*, **47**, 149−165.

Hicher, P.Y., Wahyudi, H. and Tessier, D. (1994) Micro-structural analysis of strain localization in clay. *Computers and Geotechnics*, **16**, 205−222.

Hrouda, F. (1991) Models of magnetic anisotropy variations in sedimentary thrust sheets. *Tectonophysics*, **185**, 203−210.

Hrouda, F. (1993) Theoretical models of magnetic anisotropy to strain relationship revisited. *Physics of the Earth and Planetary Interiors*, **77**, 237−249.

Hrouda, F. and Janak, F. (1976) The changes in shape of the magnetic susceptibility ellipsoid during progressive meta-morphism and deformation. *Tectonophysics*, **34**, 135−148.

Hrouda, F. and Ježek, J. (1999) Magnetic anisotropy indications of deformations associated with diagenesis. Pp. 127−137 in: *Palaeomagnetism and Diagenesis in Sediments* (D.H. Tarling and P. Turner, editors). Special publications **151**, Geological Society, London.

Kapicka, A., Hrouda, F., Petrovsk, E., and Polácek, J. (2006) Effect of plastic deformation in laboratory conditions on magnetic anisotropy of sedimentary rocks. *High Pressure*

Research, **26**, 549−553.

Liang, L., Saada, A., Figueroa, J.L., and Cope, C.T. (1997) The use of digital image processing in monitoring shear band development. *Geotechnical Testing Journal*, GTJODJ, **20**, 324−339.

Mukherji, A., Chaudhuri, A.K., and Mamtani, M.A. (2004) Regional scale strain variations in the banded iron formations of Eastern India: results from anisotropy of magnetic susceptibility studies. *Journal of Structural Geology*, **26**, 2175−2189.

Nemat-Nasser, S. and Okada, N. (2001) Radiographic and microscopic observation of shear bands in granular materials. *Geotechnique*, **51**, 753−765.

Prashant, A. and Penumadu, D. (2005) A laboratory study of normally consolidated kaolin clay. *Canadian Geotechnical Journal*, **42**, 27−37.

Rathore, J.S. (1979) Magnetic susceptibility anisotropy in the Cambrian slate belt of North Wales and correlation with strain. *Tectonophysics*, **53**, 83−97.

Read, H.E. and Hegemier, G.A. (1984) Strain softening of rock, soil and concrete − a review article. *Mechanics of Materials*, **3**, 271−294.

Saada, A.S., Bianchini, G.F., and Liang, L. (1994) Cracks, bifurcation and shear bands propagation in saturated clays. *Geotechnique*, **44**, 35−64.

Sachan, A. and Penumadu, D. (2007) Effect of microfabric on shear behavior of kaolin clay. *Journal of Geotechnical and Geoenvironmental Engineering*, **133**, 306−318.

Scarpelli, G. and Wood, D.M. (1982) Experimental observations of shear band patterns in direct shear tests. Pp. 473−484 in: *Proceedings of the IUTAM Conference on Deformation and Failure of Granular Materials*, Delft, Rotterdam, The Netherlands.

Sen, K., Majumder, S., and Mamtani, M.A. (2005) Degree of magnetic anisotropy as a strain intensity gauge in ferro-magnetic granites. *Journal of the Geological Society of London*, **162**, 583−586.

Sengupta, S. and Sengupta, A. (2004) Investigation into shear band formation in clay. *Indian Geotechnical Journal*, **34**, 141−163.

Tarling, D.H. and Hrouda, F. (1993) *The Magnetic Anisotropy of Rocks.* Chapman & Hall, London.

Tchalenko, J.S. (1968) The evolution of Kin-bands and the development of compression textures in sheared clays. *Tectonophysics*, **6**, 159−174.

Topolnicki, M., Gudehus, G., and Mazurkiewicz, B.K. (1990) Observed stress-strain behavior of remolded saturated clay under plane strain conditions. *Geotechnique*, **40**, 155−187.

Vardoulakis, I. (1980) Shear band inclination and shear modulus of sand in biaxial tests. *International Journal for Numerical and Analytical Methods in Geomechanics*, **4**, 103−119.

Vardoulakis, I., Graf, B., and Hettler, A. (1985) Shear band formation in a fine grained sand. Pp. 517−521 in: *Proceedings of the 5th International Conference on Numerical Methods in Geomechanics*, Vol. **1**, Nagoya, Japan.

Viggiani, G., Finno, R.J., and Harris, W.W. (1994) Experimental observations of strain localization in plane strain compression of a stiff clay. Pp. 189−198 in: *Localization and Bifurcation Theory for Soils and Rocks* (R. Chambon, J. Desrues, and I. Vardoulakis, editors). Balkema, Rotterdam.

Zuev, L.B., Semukhin, B.S., and Zarikovskaya, W.V. (2003) Deformation localization and ultrasonic wave propagation rate in tensile Al as a function of grain size. *International Journal of Soils & Structures*, **40**, 941−950.